

# In-situ animal behavior classification using knowledge distillation and fixed-point quantization

Reza Arablouei<sup>a,\*</sup>, Liang Wang<sup>b</sup>, Caitlin Phillips<sup>a</sup>, Lachlan Currie<sup>a</sup>, Jordan Yates<sup>a</sup>,  
Greg Bishop-Hurley<sup>b</sup>

<sup>a</sup>Data61, CSIRO, Pullenvale QLD 4069, Australia

<sup>b</sup>Agriculture and Food, CSIRO, St Lucia QLD 4067, Australia

---

## Abstract

We explore the use of knowledge distillation (KD) for learning compact and accurate models that enable classification of animal behavior from accelerometry data on wearable devices. To this end, we take a deep and complex convolutional neural network, known as residual neural network (ResNet), as the teacher model. ResNet is specifically designed for multivariate time-series classification. We use ResNet to distill the knowledge of animal behavior classification datasets into soft labels, which consist of the predicted pseudo-probabilities of every class for each datapoint. We then use the soft labels to train our significantly less complex student models, which are based on the gated recurrent unit (GRU) and multilayer perceptron (MLP). The evaluation results using two real-world animal behavior classification datasets show that the classification accuracy of the student GRU-MLP models improves appreciably through KD, approaching that of the teacher ResNet model. To further reduce the computational and memory requirements of performing inference using the student models trained via KD, we utilize dynamic fixed-point quantization (DQ) through an appropriate modification of the computational graph of the considered models. We implement both unquantized and quantized versions of the developed KD-based models on the embedded systems of our purpose-built collar and ear tag devices to classify animal behavior in situ and in real time. Our evaluations corroborate the effectiveness of KD and DQ in improving the accuracy and efficiency of in-situ animal behavior classification.

*Keywords:* animal behavior classification, deep learning, dynamic quantization, embedded systems, fix-point arithmetic, knowledge distillation.

---

## 1. Introduction

Accurate knowledge of animal behavior, which is an important indicator of health, welfare, productivity, and performance, can greatly help with efficient management of livestock or wildlife. Manual observation and recording of behavior for large numbers of animals over long periods is impractical as the associated costs or logistical challenges can be prohibitive. Therefore, classifying animal behavior using sensor data, e.g., inertial measurement data that

---

\*Corresponding author

can be collected via wearable devices such as collar or ear tags, is highly desirable (Riaboff et al., 2022).

Most existing works on animal behavior classification using sensor data, or more broadly times-series classification, can be divided into three categories, i.e., those based on hand-tuned thresholds in conjunctions with some simple statistical features in time or frequency domains, conventional feature-engineering-based approaches that involve separate procedures for crafting and calculating the features and learning the classification model, and end-to-end approaches that calculate the features and learn the classification model jointly.

The approaches within the first category, such as (Busch et al., 2017; Williams et al., 2019), generally achieve good accuracy when classification of a single behavior is concerned and are usually easy to implement on embedded systems or edge devices. However, such solutions are often unsuitable for multi-class classification due to their compounded complexity and poor performance.

The approaches falling into the second category have conventionally formed the mainstream literature regarding time-series data classification and particularly animal behavior classification from accelerometry data. Some examples are (Arablouei et al., 2021; Bagnall et al., 2015, 2017; Baydogan et al., 2013; Bostrom and Bagnall, 2015; Deng et al., 2013; Kate, 2016; Lines and Bagnall, 2015; Rahman et al., 2018; Schäfer, 2015; Smith et al., 2016). These approaches calculate various statistical features in time or frequency domains and feed them into supervised machine learning algorithms such as support vector machine, random forest, or multilayer perceptron. They usually achieve good performance in classifying multiple behaviors. Some of them are designed to be implemented on embedded systems or edge devices for in-situ inference. With these approaches, as the feature calculation and classification parts are optimized separately, the features need be carefully engineered and calculated prior to training the classification model.

In the approaches belonging to the third category, such as (Rahman et al., 2016; Kasfi et al., 2016; Peng et al., 2019, 2020; Wang et al., 2021; Arablouei et al., 2022a), there are learnable parameters in both feature calculation and classification parts of the underlying end-to-end models. Therefore, the parameters related to feature calculation are learned from data together with the classifier parameters rather than being determined separately. The downside of these approaches is their relatively high complexity as they often rely on large models, which are predominantly deep neural networks, to extract meaningful features directly from data. This can result in large memory requirement and processing time, which may prohibit deployment of such end-to-end models on embedded systems or edge devices with limited memory, computational, or energy resources.

The notion of knowledge distillation (KD), originally proposed in (Hinton et al., 2015), can help us realize accurate end-to-end classification on embedded systems or edge devices while respecting their resource limitations. With KD, we can utilize small models, which fit in memory and run in reasonable time but may not be highly accurate on their own, and let

them embody the intelligence of larger models, which are more accurate but too complex to run on target embedded systems or edge devices. KD, in principle, allows us to improve in-situ behavior classification performance at the expense of more costly off-device training.

The idea behind KD, as introduced in (Hinton et al., 2015), is to transfer knowledge from a large model, called the teacher, to a typically smaller one, called the student, without loss of validity. It involves two major steps that are 1) train the teacher model and, for each datapoint, calculate and record the teacher model’s output as predicted pseudo-probabilities corresponding to all classes and 2) train the student model using the pseudo-probabilities predicted by the teacher model (soft labels) as well as the ground truth (hard labels). The soft labels generated by the teacher model encode information about how the teacher model represents the knowledge that it extracts from the training dataset. Therefore, the soft labels help the student model benefit from the concise knowledge representation that is learned by the teacher model but is not attainable by the student model alone due to its insufficient capacity.

### *1.1. Contributions*

In this paper, we examine the use of KD for enhancing the accuracy of recurrent neural network (RNN)-based models for classifying animal behavior from accelerometry data. Our evaluations using two cattle behavior classification datasets collected during real-world animal trials show that KD can substantially improve the accuracy of the considered RNN-based student models via exploiting the knowledge distilled by accurate but cumbersome teacher models. In particular, KD can drive the classification accuracy of some student models close to that of their teacher model.

To further accelerate the procedure of inference via the models enhanced through KD, we apply dynamic fixed-point quantization (DQ) to the model parameters as well as the associated matrix-vector multiplications (MVMs). We also substitute the computationally-demanding activation functions with their more efficient approximations.

We implement the unquantized and quantized models on the embedded systems of our cattle collar and ear tags and evaluate their inference complexity. The experimental results indicate that DQ and activation function approximation substantially reduce the memory usage and latency of performing inference using the considered models without incurring any significant loss of accuracy.

We show that the considered RNN-based models, whose accuracy is enhanced via KD and complexity reduced via DQ, run smoothly on the embedded systems of our devices without straining the available memory, computational, or energy resources and hence deliver accurate in-situ and real-time classification of animal behavior. This is notwithstanding that running the large teacher models, which are used to make the considered RNN-based models more accurate through KD, on our devices is not feasible due to their high memory and computational demands.

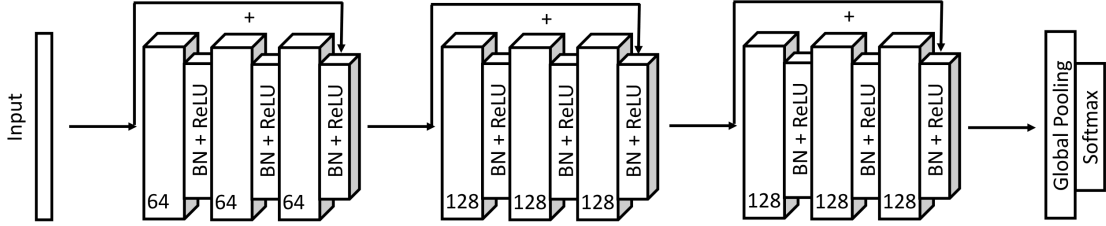


Figure 1: The architecture of the ResNet model (Wang et al., 2017).

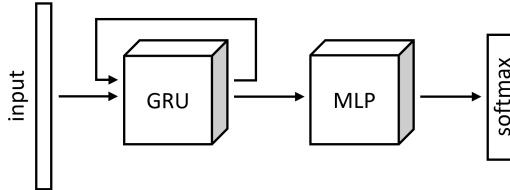


Figure 2: The architecture of the GRU-MLP models proposed in (Wang et al., 2021).

## 2. Overview of proposed approach

We employ KD to improve the accuracy of the RNN-based models proposed in (Wang et al., 2021) for animal behavior classification. We choose a nine-layer deep residual convolutional neural network, proposed in (Wang et al., 2017) for end-to-end classification of multivariate time-series data, as the teacher network. The architecture of this model, called ResNet, is sketched in Fig. 1. It is shown in (Fawaz et al., 2019) that ResNet is one of the most accurate existing time-series classification algorithms, especially among those based on neural networks.

Our student models are composed of one or two layers of the unidirectional gated recurrent unit (GRU) and a multilayer perceptron (MLP) with one hidden layer as proposed in (Wang et al., 2021). We sketch the architecture of the student models, which we call GRU-MLP, in Fig. 2. Their computational complexity and memory requirement are significantly smaller compared to the teacher model, ResNet. This is evident in Table 1 where we give the number of model parameters of the teacher and student models and the number of multiplication operations required by them for inference. As shown in Table 1, we consider three variants for the student models, which are characterized by the number of GRU layers used in them (1 or 2) and the number of hidden states in each GRU layer (32 or 64).

To improve the efficiency of performing animal behavior inference using the considered GRU-MLP models learned through KD, we apply DQ where we quantize the floating-point 32-bit (FP32) parameter values of the models into fixed-point 8-bit (Q7) numbers and convert the FP32 MVMs to their equivalent Q7 operations. To this end, we alter the computational graph of the GRU-MLP models appropriately.

To further speed up the inference via the developed models, we replace the sigmoid and hyperbolic tangent (tanh) activation functions with their rational expression (fraction of polynomials) approximations obtained via Gauss’s continued fraction with seven divisions.

Table 1: The number of parameters of the considered student and teacher models and the number of multiplication operations required by each model to perform three-class classification inference on a single datapoint made up of 256 triaxial accelerometer readings.

model	role	parameters ( $\times 10^3$ )	multiplications ( $\times 10^6$ )
GRU(1,64)-MLP	student	25.5	6.4
GRU(2,32)-MLP	student	12.9	3.2
GRU(1,32)-MLP	student	6.6	1.6
ResNet	teacher	520.2	132.6

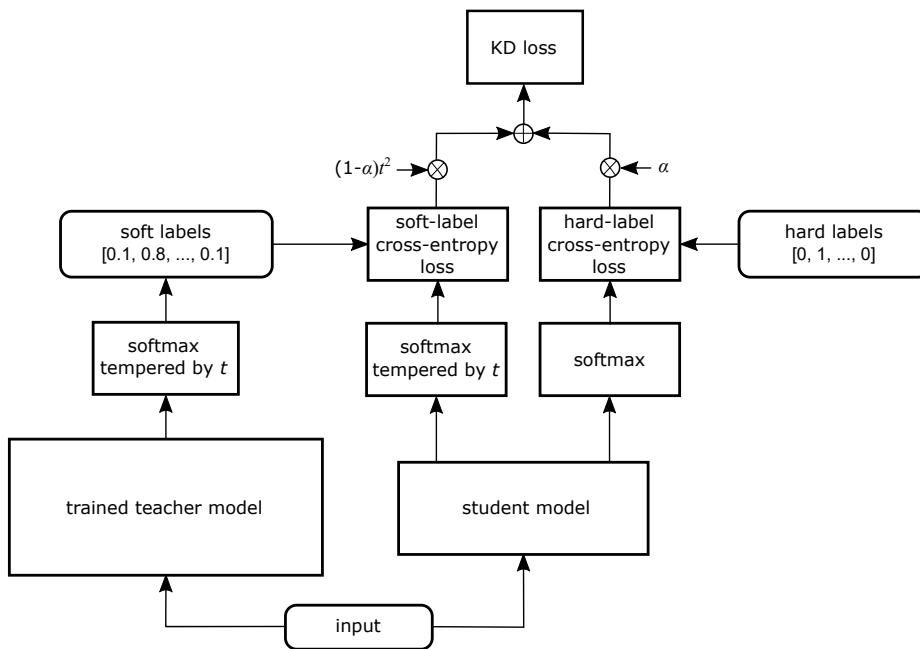


Figure 3: The diagram of calculating the KD loss when training the student model.

The approximate activation functions are significantly more efficient to compute.

We provide the detailed description of the KD and DQ processes, which we utilize in the proposed approach, in sections 3 and 4, respectively. We also present the approximation of the sigmoid and tanh functions in section 4.2.

### 3. Knowledge distillation

In this section, we provide a brief overview of the KD process that we consider in this work and describe how we set the values of the related hyperparameters.

#### 3.1. Training

The first step of the KD process is to train the teacher model followed by storing the pseudo-probabilities of all classes predicted by the trained teacher model for each datapoint in the training dataset. The pseudo-probabilities are called soft labels or soft targets and carry information on how confident the trained teacher model is about any datapoint belonging to each class. The soft labels, which can also be viewed as confidence scores, are

thought to constitute a concise representation of the knowledge within the dataset that is relevant to the classification task at hand.

The second step is to train the student model using both hard and soft labels. The difference in training of the student model brought about by KD is due to the use of the soft labels produced by the trained teacher model. Hence, the loss function associated with training the student model through KD is defined as

$$l_k = \alpha l_h + (1 - \alpha)t^2 l_s \quad (1)$$

where  $l_h$  and  $l_s$  are the loss functions corresponding to the hard and soft labels, respectively,  $\alpha$  is the mixing parameter, and  $t$  is the temperature parameter, which we will explain in the following. Fig. 3 depicts the calculation of the KD loss.

For any given datapoint, the hard-label loss function,  $l_h$ , is defined as the cross entropy of the one-hot vector of the ground-truth label and the corresponding softmax output vector of the student model, i.e.,

$$l_h = - \sum_{i=1}^C s_i \log(q_i) = - \log(q_c) \quad (2)$$

where  $s_i$  is the  $i$ th entry of the label one-hot vector,  $C$  is the number of classes,  $c$  is the index of the ground-truth class label, and  $q_i$  is the  $i$ th entry of the softmax output vector expresses as

$$q_i = \frac{\exp(z_i)}{\sum_{j=1}^C \exp(z_j)} \quad (3)$$

with  $z_i$  being the output logit corresponding to the  $i$ th class produced by the student model.

The soft-label loss function,  $l_s$ , is the cross entropy of the soft labels produced by the trained teacher model and the softmax output of the student model, both smoothed by raising the temperature from the default value of 1 to  $t > 1$  through the division of the related logits by  $t$ , i.e.,

$$l_s = - \sum_{i=1}^C p_i^{(t)} \log(q_i^{(t)}) \quad (4)$$

where

$$q_i^{(t)} = \frac{\exp\left(\frac{z_i}{t}\right)}{\sum_{j=1}^C \exp\left(\frac{z_j}{t}\right)}, \quad p_i^{(t)} = \frac{\exp\left(\frac{v_i}{t}\right)}{\sum_{j=1}^C \exp\left(\frac{v_j}{t}\right)}, \quad (5)$$

and  $v_i$  is the output logit of the trained teacher model corresponding to the  $i$ th class.

Since the gradient of  $l_s$  has an additional multiplicative factor of  $1/t^2$  compared with the gradient of  $l_h$ , we multiply the second term on the right-hand side of (1) by  $t^2$  so that the contributions of the gradients of  $l_h$  and  $l_s$  have similar orders regardless of the value of  $t$ .

### 3.2. Hyperparameters

Here, we discuss the choice of the values for two important hyperparameters involved in KD, i.e., the temperature  $t$  and the mixing parameter  $\alpha$ .

The mixing parameter  $\alpha$  governs the relative contributions of the hard-label and soft-label loss functions. If the value of  $\alpha$  is close to zero, the KD loss function is dominated by the soft-label loss function, which means the student model mainly learns to predict pseudo-probabilities similar to those of the teacher model with less emphasis on complying with the ground truth. When the value of  $\alpha$  is close to one, the KD loss function is dominated by the hard-label loss function. Hence, the agreement with ground truth is prioritized to learning from the soft labels produced by the teacher model. Since the success of KD is considered to be due to the teacher model’s ability to extract insightful information from the training dataset and encode it within the soft labels, a small value for  $\alpha$  is preferable. Our experiment results suggest that  $\alpha = 0.1$  establishes a good balance between the two loss components.

The value of the temperature  $t$  determines the relative contributions of the summand terms on the right-hand side of (4). Increasing the value of  $t$  smooths the distribution of the pseudo-probabilities in (5) and consequently increases their entropy. This allows the pseudo-probabilities with smaller values to have higher relative contribution to the soft-label loss function and therefore training via KD, which has been shown to improve the accuracy of the learned model. On the other hand, if  $t$  is too large, the pseudo-probabilities may tend to a uniform distribution and lose their information. In our experiments,  $t = 3$  appears to deliver the best results in most considered cases.

#### 4. Quantization and approximation

Our goal is to accurately classify animal behavior using accelerometry data in situ and in real time. Therefore, in this section, we explain how we utilize DQ and approximate the sigmoid and tanh activation functions to alleviate the burden of executing the considered GRU-MLP models, which are trained via KD, on the embedded systems of our collar and ear tags. In section 5, we show that DQ and the approximations substantially reduce the memory and CPU time required for on-device animal behavior inference with no significant sacrifice of classification accuracy.

To make the exposition of our ideas in this section clearer, in Algorithm 1, we summarize the procedure of performing animal behavior classification using a GRU-MLP model with a single GRU layer. In Fig. 4, we also illustrate the computational graph of the inference procedure given in Algorithm 1.

It is clear from Algorithm 1 and Fig. 4 that the most computationally demanding parts of the GRU-MLP model are the affine transformations leading to the calculation of  $\mathbf{r}_t$ ,  $\mathbf{z}_t$ , and  $\mathbf{n}_t$  together with the computation of the sigmoid and tanh activation functions.

The affine transformations represented by the blue rectangles in Fig. 4 involve the multiplication of the input or hidden state vectors by the corresponding parameter (weight) matrixes. The calculation of the MLP output also requires two affine transformations or

---

Algorithm 1: The animal behavior inference procedure using the GRU-MLP model with a single GRU layer including the related parameters.

---

input:

$\mathbf{a}_t \in \mathbb{R}^{3 \times 1}, t = 1, \dots, N$                       vectors of accelerometer readings in  $x$ ,  $y$ , and  $z$  axes  
 $\mathbf{h}_0 \in \mathbb{R}^{L \times 1}$     initial values of hidden states

output:

$c \in \{1, \dots, C\}$     predicted behavior class index

parameters:

$N \in \mathbb{Z}^+$     accelerometer reading sequence length  
 $L \in \mathbb{Z}^+$     number of hidden states  
 $C \in \mathbb{Z}^+$     number of classes  
 $\mathbf{m} \in \mathbb{R}^{3 \times 1}$     normalization means  
 $\mathbf{s} \in \mathbb{R}^{3 \times 1}$     normalization inverse standard-deviations  
 $\mathbf{W}_{ar}, \mathbf{W}_{az}, \mathbf{W}_{an} \in \mathbb{R}^{L \times 3}$                       GRU weights  
 $\mathbf{W}_{hr}, \mathbf{W}_{hz}, \mathbf{W}_{hn} \in \mathbb{R}^{L \times L}$                       GRU weights  
 $\mathbf{b}_{ar}, \mathbf{b}_{hr}, \mathbf{b}_{az}, \mathbf{b}_{hz}, \mathbf{b}_{an}, \mathbf{b}_{hn} \in \mathbb{R}^{L \times 1}$       GRU biases  
 $\mathbf{W}_1 \in \mathbb{R}^{\lfloor (L+C)/2 \rfloor \times L}, \mathbf{W}_2 \in \mathbb{R}^{C \times \lfloor (L+C)/2 \rfloor}$     MLP weights  
 $\mathbf{b}_1 \in \mathbb{R}^{\lfloor (L+C)/2 \rfloor \times 1}, \mathbf{b}_2 \in \mathbb{R}^{C \times 1}$               MLP biases

algorithm:

for  $t = 1$  to  $N$ :

    normalization:

$$\bar{\mathbf{a}}_t = (\mathbf{a}_t - \mathbf{m}) \odot \mathbf{s}$$

    uni-directional gated recurrent unit:

$$\begin{aligned} \mathbf{r}_t &= \sigma(\mathbf{W}_{ar}\bar{\mathbf{a}}_t + \mathbf{b}_{ar} + \mathbf{W}_{hr}\mathbf{h}_{t-1} + \mathbf{b}_{hr}) \\ \mathbf{z}_t &= \sigma(\mathbf{W}_{az}\bar{\mathbf{a}}_t + \mathbf{b}_{az} + \mathbf{W}_{hz}\mathbf{h}_{t-1} + \mathbf{b}_{hz}) \\ \mathbf{n}_t &= \tanh(\mathbf{W}_{an}\bar{\mathbf{a}}_t + \mathbf{b}_{an} + \mathbf{r}_t \odot (\mathbf{W}_{hn}\mathbf{h}_{t-1} + \mathbf{b}_{hn})) \\ \mathbf{h}_t &= (1 - \mathbf{z}_t) \odot \mathbf{n}_t + \mathbf{z}_t \odot \mathbf{h}_{t-1} \end{aligned}$$

    multilayer perceptron:

$$c = \arg \max(\mathbf{W}_2 \max(\mathbf{0}, \mathbf{W}_1 \mathbf{h}_N + \mathbf{b}_1) + \mathbf{b}_2)$$


---

MVMs. However, the six MVMs carried out in each iteration of every GRU layer are particularly taxing as the number of iterations is equal to the length of the input data sequence, which is 256 in our case. In addition, the weight matrixes may occupy sizable memory space when stored in full precision. The same arguments regarding the major factors of computational and memory complexity also apply to the GRU-MLP models with more than one GRU layer.

#### 4.1. Dynamic fixed-point quantization

To reduce the computational complexity of the MVMs and the memory space occupied by the weight matrixes of the GRU-MLP models, we utilize a DQ scheme where we quantize the weights to 8-bit integers and perform the MVMs via Q7 arithmetic. The main advantage of using fixed-point arithmetic operations is that they reduce the likelihood of overflow and

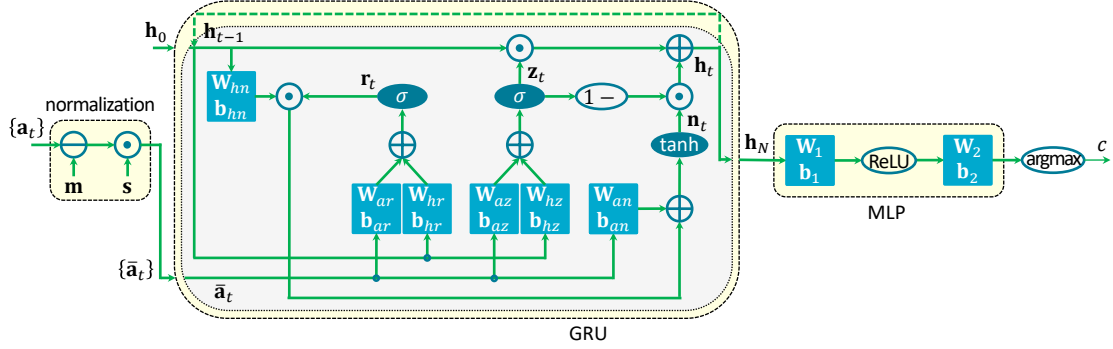


Figure 4: The computational graph of performing inference via a GRU(1,L)-MLP model.

consequent incorrect results. However, this comes at the expense of reduced precision, which is a price worth paying considering that the repercussions of overflow are often more severe compared to precision loss.

We quantize the entries of all model parameter (weight) matrixes, e.g.,  $\mathbf{W}_{ar}$  and  $\mathbf{W}_{hr}$  in Algorithm 1, which originally have FP32 values, to 8-bit integer values ranging between  $-128$  and  $127$ . To quantize each weight matrix, we use a center-point, also known as zero-point, of zero and calculate the corresponding scale parameter such that all entries of the matrix have quantized values between  $-128$  and  $127$ . Therefore, as an example, for  $\mathbf{W}_{ar}$ , we set the scale parameter to  $s_{ar} = \frac{2}{2^8-1} \max(|\mathbf{W}_{ar}|)$  where the absolute value operator,  $|\cdot|$ , and the maximum value operator,  $\max(\cdot)$ , apply entry-wise and globally, respectively. Therefore, we calculate the quantized integer values as  $\mathbf{W}_{arQ} = \lfloor s_{ar}^{-1} \mathbf{W}_{ar} \rfloor$  where  $\lfloor \cdot \rfloor$  denotes rounding to the nearest integer.

In Fig. 5(a), we depict the computational graph of calculating  $\mathbf{r}_t$  without any quantization. In Fig. 5(b), we show the modified version of this computational graph where we use the quantized integer weight matrixes, i.e.,  $\mathbf{W}_{arQ}$  and  $\mathbf{W}_{hrQ}$ , instead of the FP32 matrixes  $\mathbf{W}_{ar}$  and  $\mathbf{W}_{hr}$  and replace the FP32 MVMs with the corresponding Q7 operations. To utilize Q7 MVMs effectively, we scale the values of the input matrix and input vector appropriately so that the entries of the vector resulting from the multiplication are between  $-1$  and  $+1$ , hence the output vector can be correctly represented by Q7 numbers. Thus, we divide the values of all entries of the vectors  $\bar{\mathbf{a}}_t$  and  $\mathbf{h}_{t-1}$  by the input scale parameters denoted by  $s_a$  and  $s_h$ , respectively, to ensure that they are scaled properly before converting them to Q7 format and feeding into Q7 matrix-vector multipliers. After the multiplication, we convert the results back to the FP32 format and rescale them via multiplying by the appropriate rescaling parameters, i.e.,  $\tilde{s}_{ar} = 2^7 s_a s_{ar}$  and  $\tilde{s}_{hr} = 2^7 s_h s_{hr}$  as shown in Fig. 5(b). Multiplication by  $2^7$  is to compensate for the implicit division by  $2^7$  that occurs when inputting the 8-bit-integer-valued matrixes, such as  $\mathbf{W}_{arQ}$  and  $\mathbf{W}_{hrQ}$ , into the respective Q7 MVMs. The implicit division is due to that the Q7 MVM function presumes the entries of the quantized matrixes to be in Q7 format.

We use the same procedure to quantize the weight matrixes and reduce the complexity of

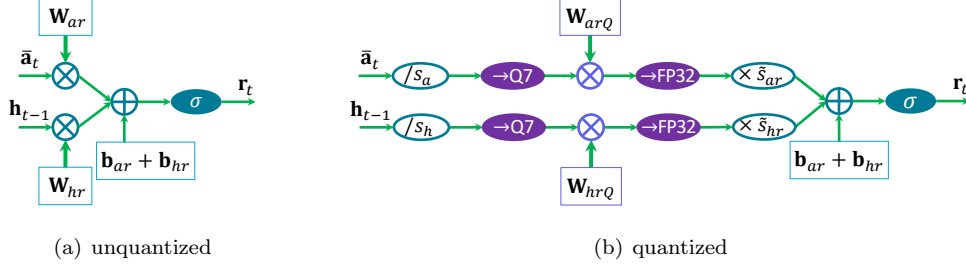


Figure 5: The computational graphs of calculating  $\mathbf{r}_t$  with and without DQ.

the MVMs involved in the calculation of  $\mathbf{z}_t$  and  $\mathbf{n}_t$  for every GRU layer and the calculation of the MLP output. We tune the input scale parameters  $s_a$  and  $s_h$  empirically to achieve the best inference results. To minimize the associated computational burden, we only consider powers-of-two values for these parameters when tuning them.

With DQ, we only store the quantized weight matrixes, which take up four times less memory compared to the original unquantized weight matrixes. Therefore, quantization can provide significant savings in memory usage, even though it incurs a small memory overhead for storing the related scale parameters. Quantization can also reduce inference latency since fixed-point arithmetic operations are generally more efficient than floating-point operations.

#### 4.2. Approximation of activation functions

Precise calculation of the sigmoid and tanh functions on embedded systems can be costly with little or no benefit in the context of machine-learning inference using neural networks. Therefore, we implement an approximate version of the tanh function using Gauss’s continued fraction with seven divisions (Gauss, 1863) that is expressed as

$$\tanh(x) \approx \frac{x}{1 + \frac{x^2}{3 + \frac{x^2}{5 + \frac{x^2}{7 + \frac{x^2}{9 + \frac{x^2}{11 + \frac{x^2}{13}}}}}} \quad (6)$$

$$\approx \frac{x^7 + 378x^5 + 17325x^3 + 135135x}{28x^6 + 3150x^4 + 62370x^2 + 135135} \quad (7)$$

and is valid for  $x \in [-4.972, 4.972]$ . For any input  $x$  outside this range, we clip the corresponding approximate tanh function value to  $-1$  or  $+1$  depending on whether  $x$  is negative or positive. Accordingly, we approximate the sigmoid function as

$$\sigma(x) = \frac{\tanh(x) + 1}{2} \quad (8)$$

$$\approx \frac{1}{2} \left( \frac{x^7 + 378x^5 + 17325x^3 + 135135x}{28x^6 + 3150x^4 + 62370x^2 + 135135} + 1 \right) \quad (9)$$

and clip it to 0 or  $+1$  when the input is outside the above-mentioned range.

## 5. Evaluation

In this section, we evaluate the classification accuracy and inference complexity of the considered GRU-MLP models that are trained via KD (with the ResNet model as the

teacher) and quantized via DQ.

### 5.1. Datasets

In our evaluations, we use two real-world datasets containing labeled accelerometry data collected during an experiment with eight grazing beef cattle. The experiment was conducted in March 2020 at the Commonwealth Scientific and Industrial Research Organisation (CSIRO) FD McMaster Laboratory Pasture In-take Facility (Greenwood et al., 2014), Chiswick NSW, Australia (30°36′28.17″S, 151°32′39.12″E). The experiments were approved by the CSIRO FD McMaster Laboratory Chiswick Animal Ethics Committee with the animal research authority numbers 19/18.

We have collected triaxial accelerometry data using custom-build collar tags<sup>1</sup> and ear tags<sup>2</sup> worn by the cattle. The sample rates of the accelerometers on the collar and ear tags were 50 Hz and 62.5 Hz, respectively. Therefore, each 256 consecutive accelerometer readings correspond to time windows of 5.12s and 4.1s for the collar and ear tags, respectively.

We have annotated parts of the collected raw accelerometry data by examining the videos of the cattle recorded during the experiment. In this work, consistent with our previous related work in (Wang et al., 2021), we consider three behavior classes of grazing, resting, and alia. The resting behavior class also includes the ruminating behavior. The alia class includes all behaviors other than grazing and resting. To avoid confusion, we use the Latin word *alia* instead of *other* to describe the class that encompasses all remaining behaviors. We refer to the datasets corresponding to the data collected via collar tags and ear tags as Arm20c and Arm20e, respectively. In both datasets, each datapoint contains 256 consecutive triaxial accelerometer readings and their associated behavior class label.

More detailed information about the experiment and the datasets as well as the hardware and software utilized for data collection can be found in (Arablouei et al., 2022a; Wang et al., 2021; Arablouei et al., 2022b).

### 5.2. Overall accuracy

We use the Matthews correlation coefficient (MCC) (Matthews, 1975) as our classification accuracy metric. The MCC is a suitable accuracy measure when the underlying dataset is imbalanced as it takes into account true and false positives and negatives. Its value is between  $-1$  and  $+1$  with  $+1$  being perfect prediction,  $0$  no better than random prediction, and  $-1$  perfect inverse prediction.

In addition, we use a leave-one-animal-out cross-validation scheme where, in each fold, we use the data of one animal for validation and the remaining data for training and tuning the relevant hyperparameters. To calculate the cross-validated MCC values, we aggregate the classification results evaluated on the validation data of all folds.

---

<sup>1</sup><https://www.csiro.au/en/research/animals/livestock/egrazor-measuring-cattle-pasture-intake>

<sup>2</sup><https://www.cerestag.com/>

Table 2: The cross-validated MCC values of the considered student models with and without KD and those of the teacher ResNet model for both considered datasets.

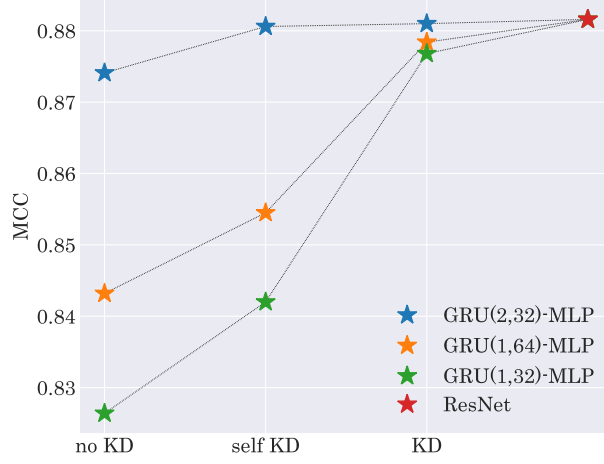
dataset	model	no KD	self KD	KD
Arm20c	GRU(2,32)-MLP	0.874	0.881	0.881
	GRU(1,64)-MLP	0.843	0.855	0.878
	GRU(1,32)-MLP	0.826	0.842	0.877
	ResNet	0.882		
Arm20e	GRU(2,32)-MLP	0.762	0.778	0.806
	GRU(1,64)-MLP	0.751	0.768	0.791
	GRU(1,32)-MLP	0.739	0.760	0.780
	ResNet	0.819		

We set the values of the hyperparameters of the ResNet model according to Table 1 of (Fawaz et al., 2019), which are shown to be optimal in different applications with various datasets.

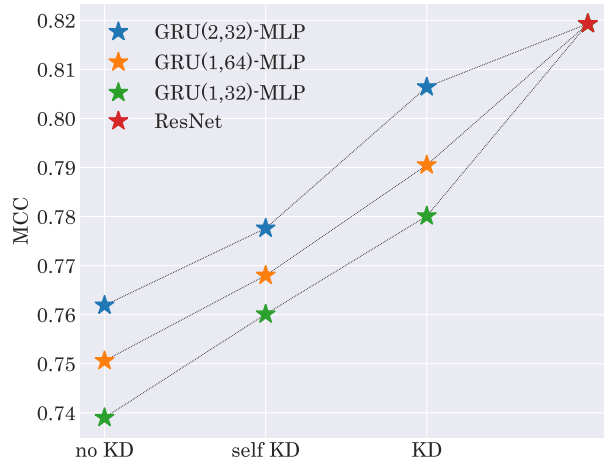
In Table 2, we present the cross-validated MCC values for the considered student GRU-MLP models when trained with and without KD and those of the teacher ResNet model for both considered datasets. The table contains the multiclass MCC values calculated by taking into account all entries of the respective confusion matrixes (Gorodkin, 2004). The results for the models trained without any KD are in the *no KD* column and those for the models trained via KD are in the *KD* column. The *self KD* column contains the results for the models that are trained via KD while each model is its own teacher. To facilitate comparison, in Fig. 6, we provide a visual representation of the MCC values given in Table 2.

The results in Table 2 and Fig. 6 demonstrate that KD appreciably improves the classification accuracy for all considered models and datasets. The improvement due to KD with the ResNet model is significant when evaluated over both datasets. However, it is more pronounced with the Arm20c dataset, where KD drives the MCC values of all three GRU-MLP models close to that of the teacher ResNet model. The accuracy improvement offered by KD with the Arm20e dataset appears to be not as noticeable as that with the Arm20c dataset. However, KD is still significantly helpful with the Arm20e dataset as classifying animal behavior using ear tag accelerometry data is inherently more challenging compared to using collar tag data (Wang et al., 2021; Arablouei et al., 2022b).

As expected, KD using the ResNet model as the teacher is more effective compared with using the GRU-MLP models as their own teachers. However, the results suggest that there still exists substantial benefits to KD, even when the GRU-MLP models teach themselves. This attests to the efficacy of KD in providing a more practical classification target through the use of soft labels, even if they do not come from a more accurate teacher model. In addition, self KD appears to be more effective when the models are learned from the Arm20e dataset. This may also be attributable to the comparatively higher complexity of recognizing



(a) The Arm20c dataset.



(b) The Arm20e dataset.

Figure 6: The cross-validated MCC values of the considered student models with and without KD and those of the teacher ResNet model for both considered datasets.

animal behavior from ear tag accelerometry data.

### 5.3. Accuracy for each behavior

In Table 3, we provide the cross-validated MCC values corresponding to each considered behavior class for all considered models with or without KD and for both considered datasets. The per-class MCC values are calculated by treating the classification of each behavior class as a binary classification problem.

Grazing is the most common behavior observed in grazing beef cattle. It is also the most prevalent behavior in our datasets, which represent the real life rather well. The grazing behavior leaves a distinct signature in triaxial accelerometry data, particularly the data collected by collar tags. This is mainly because during grazing the animal lowers its head and moves it relatively vigorously. Therefore, the considered GRU-MLP models can classify the grazing behavior with good accuracy even without KD. Nevertheless, KD improves the accuracy of classifying the grazing behavior, especially with the Arm20e dataset

Table 3: The cross-validated MCC values corresponding to each considered behavior class for all considered models with and without KD and for both considered datasets.

dataset	behavior	model	no KD	self KD	KD
Arm20c	grazing	GRU(2,32)-MLP	0.908	0.909	0.909
		GRU(1,64)-MLP	0.898	0.906	0.909
		GRU(1,32)-MLP	0.884	0.898	0.908
		ResNet	0.909		
	resting	GRU(2,32)-MLP	0.908	0.911	0.918
		GRU(1,64)-MLP	0.874	0.884	0.914
		GRU(1,32)-MLP	0.868	0.877	0.912
		ResNet	0.920		
	alia	GRU(2,32)-MLP	0.750	0.755	0.765
		GRU(1,64)-MLP	0.700	0.718	0.763
		GRU(1,32)-MLP	0.666	0.688	0.757
		ResNet	0.766		
Arm20e	grazing	GRU(2,32)-MLP	0.851	0.862	0.880
		GRU(1,64)-MLP	0.834	0.856	0.872
		GRU(1,32)-MLP	0.835	0.853	0.870
		ResNet	0.895		
	resting	GRU(2,32)-MLP	0.786	0.810	0.831
		GRU(1,64)-MLP	0.784	0.807	0.819
		GRU(1,32)-MLP	0.782	0.804	0.812
		ResNet	0.839		
	alia	GRU(2,32)-MLP	0.534	0.537	0.604
		GRU(1,64)-MLP	0.539	0.543	0.577
		GRU(1,32)-MLP	0.500	0.522	0.558
		ResNet	0.638		

and the models that have a single GRU layer, i.e., GRU(1,32)-MLP and GRU(1,64)-MLP. Using the Arm20c dataset and the ResNet model as the teacher, the per-class MCC values corresponding to the grazing behavior approach that of the ResNet model for all considered student models trained via KD.

Classification of the resting and alia behavior classes is more challenging compared to the grazing behavior. The resting behavior, which here includes the ruminating behavior, may occasionally be confused with other behaviors that occur with low levels of animal body motion, such as drinking or searching, which are considered to fall into the alia behavior class.

Overall, the results of Table 3 show that KD can significantly improve the classification accuracy of all considered behavior classes with both collar and ear tag accelerometry data.

#### 5.4. Accuracy of quantized models

Here, we evaluate the accuracy of classifying animal behavior via the quantized models over both Arm20c and Arm20e datasets and present the resulting cross-validated MCC

Table 4: The cross-validated MCC values for both unquantized and quantized versions of the considered models trained via KD with ResNet as the teacher and for both considered datasets, and the difference between the MCC values of the unquantized and quantized versions for each model.

dataset	model	unquantized	quantized	difference
Arm20c	GRU(2,32)-MLP	0.881	0.874	0.007
	GRU(1,64)-MLP	0.855	0.851	0.004
	GRU(1,32)-MLP	0.842	0.839	0.003
Arm20e	GRU(2,32)-MLP	0.778	0.772	0.006
	GRU(1,64)-MLP	0.768	0.765	0.003
	GRU(1,32)-MLP	0.760	0.758	0.002

values in Table 4 together with the MCC values for the unquantized models. In Table 4, we also give the difference between the cross-validated MCC values of the unquantized and quantized versions of each model. As seen in Table 4, the difference between the MCC values of the unquantized and quantized versions of all models is small. Therefore, the loss of classification accuracy due to dynamic fix-point quantization is practically negligible for all considered GRU-MLP models.

### 5.5. Complexity of in-situ inference

We implement performing inference using both unquantized and quantized versions of the considered student models containing one or two GRU layers on the embedded systems of our bespoke cattle collar and ear tags and evaluate their memory usage and on-device runtime.

We implement the considered GRU-MLP models trained via KD on the embedded systems of our collar and ear tags for inferring animal behavior in situ and in real time. To evaluate the savings afforded by DQ in terms of memory usage and CPU runtime, we implement both unquantized and quantized versions of each model. Our target embedded system utilizes a Nordic nRF52840<sup>3</sup> system-on-chip microcontroller containing a 64MHz ARM Cortex-M4F CPU, 256kB of random-access memory (RAM), 1MB of flash read-only memory (ROM), and a floating-point unit (FPU).

In our implementations, we use the Arm Common Microcontroller Software Interface Standard (CMSIS)’s DSP and NN libraries<sup>4</sup> and the Zephyr real-time operation system<sup>5</sup>. CMSIS is a vendor-independent abstraction layer for microcontrollers that are based on Arm Cortex processors.

In Table 5, we provide the required memory and CPU runtime of performing inference on a single datapoint, i.e., 256 consecutive triaxial accelerometer readings, using both un-

<sup>3</sup><https://www.nordicsemi.com/products/nrf52840>

<sup>4</sup><https://developer.arm.com/tools-and-software/embedded/cmsis>

<sup>5</sup><https://www.zephyrproject.org/>

Table 5: The complexity of performing on-device inference using the consider GRU-MLP models with and without quantization in terms of CPU time and memory usage.

	model	CPU time (ms)	rodata (kB)	text (kB)	stack (kB)
unquantized	GRU(2,32)-MLP	723	41.80	3.28	2.85
	GRU(1,64)-MLP	892	62.02	2.76	2.91
	GRU(1,32)-MLP	286	16.71	2.76	2.26
quantized	GRU(2,32)-MLP	314	11.29	4.23	3.47
	GRU(1,64)-MLP	371	16.39	3.55	4.35
	GRU(1,32)-MLP	139	4.63	3.55	2.33

quantized and quantized versions of the considered GRU-MLP models. The terms “text” and “rodata” refer to the ROM space occupied by the algorithm code and the model parameters, respectively, while “stack” refers to the RAM space required to store all variables when running each model.

The results in Table 5 show that the runtime of each quantized model is less than half of that of its unquantized counterpart. In addition, although quantization slightly increase the RAM usage, it yields considerable reduction in ROM usage.

During a field trial with eight Angus beef cows in February 2022, we performed in-situ behavior classification on the embedded systems of our collar and ear tags using both unquantized and quantized versions of the considered GRU-MLP models, which were trained via KD over the Arm18 and Arm20 datasets. All models ran effectively in real time inferring cattle behavior with classification accuracy on par with the results presented in Table 2.

## 6. Concluding remarks

Using end-to-end deep learning models such as ResNet, animal behavior can be classified accurately from accelerometry data collected by wearable sensors. Deep neural networks have high learning ability owing to their aptly-crafted deep and complex architectures. However, they are large and resource-hungry hence not suitable for implementation on embedded systems or edge devices, which have limited computational, memory, and energy resources. The notion of KD allows the knowledge gained by a complex and accurate model to be transferred to a less complex one that demands less resources and can be implemented on embedded systems or edge devices for in situ and real time inference. As a result, KD enhances the accuracy of classification models that are suitable for on-device inference by utilizing the knowledge acquired from training datasets through more accurate and complex teacher models. KD enables more accurate inference via low-complexity models at the cost of more laborious training. Therefore, KD essentially allows trading training complexity for inference accuracy and simplicity.

Our findings corroborate the merits of KD, even in its most fundamental form, i.e., utilizing soft labels. It enables accurate on-device classification of animal behavior using

accelerometry time-series data through imparting the knowledge of a complex model such as ResNet to less complex ones such as GRU-MLP by means of the soft labels generated by the ResNet model. KD is effective even when a GRU-MLP model is used as its own teacher. This points to the fundamental shortcomings of the cross-entropy loss with hard labels in training classification models. When a classification model has restricted learning capacity and the amount of training data is limited, estimating the model’s parameters through optimizing the cross-entropy loss with hard labels may become a highly underdetermined problem. Having less strict and more nuanced soft labels as the classification target instead of the hard labels may alleviate this problem thanks to the additional information afforded by the soft labels. This is possible even when the soft labels are produced by the student model itself and not a more accurate teacher model.

We use two real-world datasets collected via cattle collar and ear tags to validate the advantages of KD and quantization for on-device animal behavior classification using accelerometry data. The two datasets have substantial dissimilarities since the utilized collar and ear tags are worn by the cattle differently, i.e., on top of the animal’s neck versus on its ear, and have different accelerometer chips with different sampling rates. Thus, the considered models perform considerably differently when evaluated using different datasets. This also applies to the accuracy improvement due to KD. However, regardless of the dataset used, the advantages of KD are evident, albeit to varying degrees. In addition, it appears that, the more challenging a particular behavior is to classify correctly, the more KD improves its classification accuracy.

Our evaluations attest to the effectiveness of DQ in reducing the inference time and memory requirement of the considered GRU-MLP models. The benefits of quantization come with no significant loss in classification accuracy. The savings in inference latency and memory usage offered by quantization are critical when the inference is implemented on resource-constrained devices involving embedded systems or edge devices. DQ provides significant reduction in runtime by cutting it almost in half, despite the utilized microcontroller being equipped with an FPU. This can be attributed to the fact that 8-bit DQ allows Cortex-M4 CPU to utilize the single instruction multiple data (SIMD) feature since Q7 arithmetic operations are performed on 8-bit (one-byte) numbers while FP32 operations are performed on 32-bit (4-byte) numbers. SIMD enables multiple 8-bit or 16-bit operations in a single cycle, i.e., simultaneous computation of two 16-bit or four 8-bit operands, with a near zero increase in power consumption (Martin, 2016).

It is noteworthy that, despite leading to a significant decrease in the precision of the model parameters and the related MVMs, DQ has little effect on the classification accuracy of the considered GRU-MLP models. The GRU entails a recursive procedure that may result in propagation and accumulation of quantization errors. However, the quantization errors accumulate only to a limited extent over the initial iterations, after which the associated cumulative error plateaus. This is likely because the quantization errors are distributed

symmetrically around zero hence cancel out statistically when added together.

In this work, we only considered dynamic quantization where only the model weight matrixes are quantized. Dynamic quantization is favorable when loading the weight matrixes from the memory constitutes a significant portion of the model execution time. It is generally the preferred method to quantize recurrent neural network such as GRU. In future work, we will examine the use of static quantization where both model parameters and activations are quantized. We will also consider quantization-aware training by modeling the effects of quantization during training.

## Acknowledgments

This research was undertaken with strategic investment funding from the CSIRO and NSW Department of Primary Industries. We would like to thank the technical staff who were involved in the research at CSIRO FD McMaster Laboratory Chiswick, i.e., Flavio Alvarenga, Alistair Donaldson, and Reg Woodgate of the NSW Department of Primary Industries, and Jody McNally and Troy Kalinowski of the CSIRO Agriculture and Food. We also recognize the contributions of the CSIRO Data61 staff who have designed and built the hardware and software of the devices used for data collection, specifically, John Scolaro, Leslie Overs, and Stephen Brosnan.

## References

- Arablouei, R., Currie, L., Kusy, B., Ingham, A., Greenwood, P.L., Bishop-Hurley, G., 2021. In-situ classification of cattle behavior using accelerometry data. *Computers and Electronics in Agriculture* 183, 106045.
- Arablouei, R., Wang, L., Currie, L., Alvarenga, F.A.P., Bishop-Hurley, G.J., 2022a. Animal behavior classification via deep learning on embedded systems. *arXiv preprint arXiv:2111.12295* .
- Arablouei, R., Wang, Z., Bishop-Hurley, G.J., Liu, J., 2022b. Multi-modal sensor data fusion for in-situ classification of animal behavior using accelerometry and gnss data. *arXiv preprint arXiv:2206.12078* .
- Bagnall, A., Lines, J., Bostrom, A., Large, J., Keogh, E., 2017. The great time series classification bake off: a review and experimental evaluation of recent algorithmic advances. *Data Mining and Knowledge Discovery* 31, 606–660.
- Bagnall, A., Lines, J., Hills, J., Bostrom, A., 2015. Time-series classification with cote: the collective of transformation-based ensembles. *IEEE Transactions on Knowledge and Data Engineering* 27, 2522–2535.
- Baydogan, M.G., Runger, G., Tuv, E., 2013. A bag-of-features framework to classify time series. *IEEE transactions on pattern analysis and machine intelligence* 35, 2796–2802.

- Bostrom, A., Bagnall, A., 2015. Binary shapelet transform for multiclass time series classification, in: International conference on big data analytics and knowledge discovery, Springer. pp. 257–269.
- Busch, P., Ewald, H., Stüpmann, F., 2017. Determination of standing-time of dairy cows using 3d-accelerometer data from collars, in: 2017 Eleventh International Conference on Sensing Technology (ICST), IEEE. pp. 1–4.
- Deng, H., Runger, G., Tuv, E., Vladimir, M., 2013. A time series forest for classification and feature extraction. *Information Sciences* 239, 142–153.
- Fawaz, H.I., Forestier, G., Weber, J., Idoumghar, L., Muller, P.A., 2019. Deep learning for time series classification: a review. *Data Mining and Knowledge Discovery* 33, 917–963.
- Gauss, C.F., 1863. *Werke*. volume 3. Göttingen.
- Gorodkin, J., 2004. Comparing two k-category assignments by a k-category correlation coefficient. *Computational Biology and Chemistry* 28, 367–374.
- Greenwood, P.L., Valencia, P., Overs, L., Paull, D.R., Purvis, I.W., 2014. New ways of measuring intake, efficiency and behaviour of grazing livestock. *Animal Production Science* 54, 1796–1804.
- Hinton, G., Vinyals, O., Dean, J., 2015. Distilling the knowledge in a neural network. arXiv preprint arXiv:1503.02531 .
- Kasfi, K.T., Hellicar, A., Rahman, A., 2016. Convolutional neural network for time series cattle behaviour classification, in: Proceedings of the Workshop on Time Series Analytics and Applications, pp. 8–12.
- Kate, R.J., 2016. Using dynamic time warping distances as features for improved time series classification. *Data Mining and Knowledge Discovery* 30, 283–312.
- Lines, J., Bagnall, A., 2015. Time series classification with ensembles of elastic distance measures. *Data Mining and Knowledge Discovery* 29, 565–592.
- Martin, T., 2016. *The Designer’s Guide to the Cortex-M Processor Family*. Newnes.
- Matthews, B.W., 1975. Comparison of the predicted and observed secondary structure of t4 phage lysozyme. *Biochimica et Biophysica Acta (BBA)-Protein Structure* 405, 442–451.
- Peng, Y., Kondo, N., Fujiura, T., Suzuki, T., Ouma, S., Yoshioka, H., Itoyama, E., et al., 2020. Dam behavior patterns in japanese black beef cattle prior to calving: Automated detection using lstm-rnn. *Computers and Electronics in Agriculture* 169, 105178.
- Peng, Y., Kondo, N., Fujiura, T., Suzuki, T., Yoshioka, H., Itoyama, E., et al., 2019. Classification of multiple cattle behavior patterns using a recurrent neural network with

- long short-term memory and inertial measurement units. *Computers and Electronics in Agriculture* 157, 247–253.
- Rahman, A., Smith, D., Hills, J., Bishop-Hurley, G., Henry, D., Rawnsley, R., 2016. A comparison of autoencoder and statistical features for cattle behaviour classification, in: 2016 international joint conference on neural networks (IJCNN), IEEE. pp. 2954–2960.
- Rahman, A., Smith, D., Little, B., Ingham, A., Greenwood, P., Bishop-Hurley, G., 2018. Cattle behaviour classification from collar, halter, and ear tag sensors. *Information processing in agriculture* 5, 124–133.
- Riaboff, L., Shalloo, L., Smeaton, A.F., Couvreur, S., Madouasse, A., Keane, M.T., 2022. Predicting livestock behaviour using accelerometers: A systematic review of processing techniques for ruminant behaviour prediction from raw accelerometer data. *Computers and Electronics in Agriculture* 192, 106610.
- Schäfer, P., 2015. The boss is concerned with time series classification in the presence of noise. *Data Mining and Knowledge Discovery* 29, 1505–1530.
- Smith, D., Rahman, A., Bishop-Hurley, G.J., Hills, J., Shahriar, S., Henry, D., Rawnsley, R., 2016. Behavior classification of cows fitted with motion collars: Decomposing multi-class classification into a set of binary problems. *Computers and Electronics in Agriculture* 131, 40–50.
- Wang, L., Arablouei, R., Alvarenga, F.A.P., Bishop-Hurley, G.J., 2021. Animal behavior classification via accelerometry data and recurrent neural networks. arXiv preprint arXiv:2111.12843 .
- Wang, Z., Yan, W., Oates, T., 2017. Time series classification from scratch with deep neural networks: A strong baseline, in: 2017 International joint conference on neural networks (IJCNN), IEEE. pp. 1578–1585.
- Williams, L.R., Bishop-Hurley, G.J., Anderson, A.E., Swain, D.L., 2019. Application of accelerometers to record drinking behaviour of beef cattle. *Animal Production Science* 59, 122–132.